NASA TECHNICAL MEMORANDUM

NASA TM X-1499

NASA TM X-1499

PERFORMANCE OF A 19.7-METER-DIAMETER DISK-GAP-BAND PARACHUTE IN A SIMULATED MARTIAN ENVIRONMENT

by Richard J. Bendura, Earle K. Huckins III, and Lucille C. Coltrane

Langley Research Center
Langley Station, Hampton, Va.

NATIONAL AERONAUTICS AND SPACE ADMINISTRATION • WASHINGTON, D. C. • JANUARY 1968

NASA TM X-1499

PERFORMANCE OF A 19.7-METER-DIAMETER DISK-GAP-BAND PARACHUTE IN A SIMULATED MARTIAN ENVIRONMENT

By Richard J. Bendura, Earle K. Huckins III,
and Lucille C. Coltrane

Langley Research Center
Langley Station, Hampton, Va.

Technical Film Supplement L-983 available on request

NATIONAL AERONAUTICS AND SPACE ADMINISTRATION

For sale by the Clearinghouse for Federal Scientific and Technical Information
Springfield, Virginia 22151 – CFSTI price $3.00

PERFORMANCE OF A 19.7-METER-DIAMETER DISK-GAP-BAND PARACHUTE IN A SIMULATED MARTIAN ENVIRONMENT

By Richard J. Bendura, Earle K. Huckins III,
and Lucille C. Coltrane
Langley Research Center

SUMMARY

Inflation and drag characteristics of a 64.7-foot (19.7-meter) nominal-diameter disk-gap-band parachute deployed at a Mach number of 1.59 and a dynamic pressure of 11.6 psf (555 N/m^2) were obtained from the second balloon-launched flight test of the Planetary Entry Parachute Program. In addition, parachute stability characteristics during the subsonic descent portion of the test are presented. After deployment, the parachute rapidly inflated to a full condition, partially collapsed, and then reinflated to a stable configuration. After reinflation, an average drag coefficient of about 0.55 based on nominal surface area was obtained. The parachute exhibited good stability characteristics during descent. The only major damage to the parachute during the test was the tearing of two canopy panels; a loss of less than 0.5 percent of nominal surface area resulted.

INTRODUCTION

The NASA Planetary Entry Parachute Program (PEPP) was established to provide test data on several parachute configurations for space flight applications, such as the Voyager mission. Such applications require performance characteristics in a low-density environment. Large-scale flight testing of parachutes deployed behind blunt bodies at supersonic speeds was undertaken because no test facilities suitable for investigating this application existed. In addition, little confidence existed in extrapolating large-scale parachute characteristics from small-scale parachute data. The combination of parachute size, deployment Mach number, and density environment was outside the limits of applicable experience.

Flight tests which simulate conditions expected in the Martian atmosphere during parachute operation have been conducted by using both rocket-launched and balloon-launched spacecraft. (See ref. 1.) Modified ringsail, disk-gap-band, and cross parachutes have been tested. References 2 to 4 present the results published from the

rocket-launched tests, and reference 5 shows the data from the first flight of the balloon-launched series.

The present document describes the basic test results obtained from the second flight test of the balloon-launched series of the Planetary Entry Parachute Program. Specifically, the inflation, drag, and stability characteristics are presented for a 64.7-foot (19.7-meter) nominal-diameter disk-gap-band parachute deployed in the wake of a 15-foot-diameter (4.6-meter) spacecraft. The parachute was deployed at a Mach number of 1.59 and a dynamic pressure of 11.6 lb/ft^2 (555 N/m^2). Little analysis is presented in order to expedite publication of the basic data.

A 16-millimeter motion-picture film supplement showing the parachute inflation sequence photographed from onboard cameras is available on loan.

SYMBOLS

a_l	linear acceleration along body longitudinal axis, g units (1g = 9.807 meters per second^2)
$C_{D,o}$	drag coefficient, Drag/$q_\infty S_o$
$(C_{D,o})_{eff}$	effective drag coefficient, $2W/\rho_\infty S_o \dot{Z}_E^2$
D_o	nominal diameter, $\left(\frac{4}{\pi} S_o\right)^{1/2}$, feet (meters)
g	acceleration due to gravity, feet per second^2 (meters per second^2)
M	Mach number
q_∞	free-stream dynamic pressure, pounds per foot^2 (newtons per meter^2)
S_o	nominal surface area of canopy including gap and vent, foot^2 (meter^2)
T	tensiometer force, pounds (newtons)
t	onboard time, seconds
W	weight, pounds (kilograms)
X,Y,Z	body-axis system

X_E, Y_E, Z_E earth-fixed axis system

ρ_∞ free-stream upper air density, slugs per foot^3 (kilograms per meter^3)

θ, ϕ, ψ payload attitude angles relative to earth-fixed axis system, radians or degrees

δ payload resultant pitch-yaw angle from the local vertical, radians or degrees

Dots over symbols denote differentiation with respect to time. Velocities, dynamic pressures, and Mach numbers are free-stream values unless otherwise noted.

PARACHUTE DESCRIPTION

The characteristics of the fully inflated parachute are as follows:

Parachute type	Disk-gap-band	
Nominal diameter	64.68 ft	(19.71 m)
Projected diameter (during descent)	42.1 ft	(12.8 m)
Nominal total area	3288.2 ft^2	(305.5 m^2)
Disk area	1784.7 ft^2	(165.8 m^2)
Gap area	391.9 ft^2	(36.4 m^2)
Band area	1111.6 ft^2	(103.3 m^2)
Vent area	14.7 ft^2	(1.37 m^2)
Projected area (during descent)	1392.0 ft^2	(129.3 m^2)
Number of gores	72	
Total geometric porosity (as fabricated)	12.35 percent	
Porosity provided by gap	11.9 percent	
Porosity provided by vent	0.45 percent	
Total geometric porosity considering flight damage	12.80 percent	
Number of suspension lines	72	
Length of suspension lines	65.85 ft	(20.07 m)
Weight (canopy, suspension lines, and riser)	79.56 lb	(36.08 kg)

Average disk-gap-band parachute gore dimensions and the parachute-payload configuration are shown in figure 1. The dimensions presented are an average of the actual measurements of all 72 gores.

All parachute structural fabric material including lines, reinforcing tapes, webbing, and threads were fabricated from dacron. The disk material weighed 1.5 oz/yd^2 (50.9 gram/m^2) and the band weighed 1.0 oz/yd (33.9 gram/m^2). The disk portion of each gore consisted of five dacron panels and the band portion, two dacron panels. The material warp and fill threads joining the sections ran 45^o to the center line of the gore.

The test parachute was similar to but larger than the system discussed in reference 3. The canopy vent edge was reinforced with three layers of 3/4-inch-wide (1.9-cm) dacron tape of 550-pound (2450-N) rated tensile strength. The outer edge of the disk portion of the canopy and both edges of the band were reinforced with a single 3/4-inch-wide (1.9-cm) 550-pound (2450-N) rated tensile strength dacron tape. The gore edges were joined by a french fell seam and reinforced with a 3/4-inch-wide (1.9-cm) radial tape of 550-pound (2450-N) rated tensile strength dacron. Each radial tape was continuous up to the full length of the gore, across the vent, and down the gore seam on the opposite side of the canopy. At the lower edge of the band the radial tape formed a loop and was sewn back 4 inches (10 cm) on the inside surface of the band. This loop was used for attachment of the suspension lines.

The radial tapes across the gap between the band and the disk were reinforced with 3/4-inch-wide (1.9-cm) 300-pound (1330-N) rated tensile strength dacron tape. The parachute seams were strengthened with a single 3/4-inch-wide (1.9-cm) 300-pound (1330-N) rated tensile strength dacron cross-seam reinforcing tape. The parachute was designed and built under NASA contract NAS 1-6703.

The parachute-payload attachment system consisted of a riser, a tensiometer, and a bridle. The riser was fabricated of six layers of $1\frac{3}{4}$-inch-wide (4.4-cm), low elongation 7000-pound (31 000-N) rated dacron webbing. The layers separated into six legs at the confluence point and each leg joined 12 suspension lines. The bridle was constructed of 6 layers of 10 000-pound (44 500-N) rated nylon webbing which separated into 3 legs of two layers each to form attachment points on the payload. The riser and bridle were joined by a tensiometer. Together the tensiometer and bridle weighed approximately 10 pounds mass (4.5 kg).

The parachute was packed to a density of 40 pounds per cubic foot (640 kg/m^3) in a cylindrical dacron bag. The bag was lined with teflon-coated fabric to prevent abrasion. No canopy or suspension line holders or restraints were used inside the deployment bag except for a break line from the apex of the canopy to the top of the bag. Also attached to the top of the bag was a mortar lid and steel ballast. The combined weight of the deployment bag, mortar lid, and ballast was approximately 6 pounds mass (2.7 kg).

The packed parachute (not including the bridle, tensiometer, mortar lid, or ballast) was subjected to the heating process as part of a proposed sterilization procedure for equipment to be used in interplanetary atmospheric entry mission. The parachute was

exposed to a temperature of 125° C for 90 hours including the approximately 30 hours required to bring all parachute material up to the test temperature. The parachute was subjected to this high-temperature environment so that any resulting material degradation would exist during the flight test.

TEST SYSTEM DESCRIPTION

The test system consisted of a 15-foot-diameter (4.6-meter) spacecraft (see fig. 2) which was lifted to an altitude near 130 000 feet (39 600-m) by a 26 000 000-ft^3 (736 000-m^3) balloon system. The balloon system was furnished and launched by the U.S. Air Force Cambridge Research Laboratories. The principal components of the spacecraft were an aeroshell, the payload, and the test parachute.

Onboard instrumentation included five motion-picture cameras, four accelerometers, and a tensiometer. Camera 1 had a frame rate of approximately 350 frames per second and viewed the inflation process. Cameras 2 and 3 had a frame rate of 16 frames per second; camera 2 was used to determine payload motions from photographs of the horizon, and camera 3 photographed the inflation process. The aeroshell cameras (cameras 4 and 5) had a frame rate of 64 frames per second and photographed both the inflation process and payload separation from the aeroshell. Deceleration loads were recorded on ±5g and ±50g longitudinal accelerometers located in the payload. Normal and transverse accelerometers (±1g) were also positioned in the payload. A tensiometer (0 to 20 000 lb or 0 to 89 000 N) was located between the bridle and the riser lines. All accelerometer and tensiometer data were recorded by an onboard tape recorder. Both the tape recorder and camera data were obtained after recovery of the payload and aeroshell. Both the aeroshell and payload contained radar tracking beacons in addition to radio beacons which aided in recovery operations. Radar and optical tracking data for portions of the flight were provided by the White Sands Missile Range.

The aeroshell was a 120° total-angle blunt cone with a diameter equal to 15 feet (4.6 m). Its construction was similar to that described in reference 6 except that eight Titan IIIC staging rocket motors were substituted in place of the 12 Falcon M58A2 rocket motors used in that test. The purpose of this modification was to provide deployment at supersonic velocities instead of transonic conditions.

The payload configuration resembled a 45° frustum-cylinder with a diameter ratio of 0.384. Length and diameter of the cylinder were 3.24 feet (0.99 meter) and 1.77 feet (0.54 meter), respectively. Mass properties of the suspended payload were:

Weight	467.14 lb	(211.9 kg)
Center of gravity	0.86 ft	(0.26 m)
Pitch inertia	45.22 slug-ft^2	(61.27 kg-m^2)

Yaw inertia . . . . . 44.76 slug-ft^2 (60.65 kg-m^2)
Roll inertia . . . . . 4.96 slug-ft^2 (6.72 kg-m^2)

The payload center of gravity is measured rearward from the front of the frustum-cylinder juncture. Parachute bridle attachment points were located radially 0.66 foot (0.20 meter) from the longitudinal axis, 3.18 feet (0.97 meter) from the frustum-cylinder, and were equally spaced about the circumference of the payload.

The disk-gap-band parachute was packed into a cylindrical dacron bag and inserted into an ejection mortar and rested on a sabot (ejection piston) at the bottom of the mortar. The mortar cover, which was fastened to the top of the bag, closed the mortar and held the packed parachute in place. The mortar, which was approximately 12 inches (31 centimeters) in diameter and 31 inches (79 centimeters) in length, was designed to eject the packed parachute at an initial velocity of 130 fps (40 mps). A circular knife located on the parachute riser was used to cut the parachute bag mouth tie after the bag was ejected from the payload. The parachute was packed so that the suspension lines deployed before the canopy. When the suspension lines were fully extended, the combined inertia of the mortar cover, ballast, and parachute bag served to separate the parachute canopy from the bag.

The payload was secured inside the aeroshell prior to deployment by an explosive nut. Approximately $\frac{1}{2}$ second after mortar fire, the explosive nut was ignited in order to allow separation of the two items. During parachute inflation, the payload was extracted from the rear of the aeroshell, and the parachute-payload combination flew a separate trajectory from the aeroshell. The mission profile is shown in figure 3.

TEST ENVIRONMENT

The balloon-spacecraft system was launched from Walker Air Force Base, Roswell, New Mexico, on July 28, 1967, by using the balloon launch technique described in reference 6. About 3 hours after launch, the system had reached an altitude of 130 000 ft (39 600 m) and had drifted over the desired release point at White Sands Missile Range, New Mexico. Approximately 3.8 seconds after release, the rocket motors ignited and subsequently propelled the spacecraft to supersonic velocities. Shortly after burnout, deployment occurred when the mortar fired (onboard time, 7.8 seconds). The data period for parachute testing began at this time and extended until $t = 170$ seconds.

Atmospheric conditions were obtained from the results of an Arcasonde sounding rocket flight which took place about $1\frac{1}{2}$ hours after spacecraft release from the balloon system. Atmospheric density and pressure conditions obtained from these data and assumed to exist during the test are compared with 1962 standard atmosphere values in figures 4 and 5, respectively. Wind velocity and direction data are presented in figure 6.

Either radar or optical tracking data were obtained for most of the flight, and the trajectory of the parachute-payload combination is shown in figure 7. However, for the time periods corresponding to the dotted curves in figures 7, 8, and 9, no radar or optical tracking data exist. Consequently, the dotted-line portions of these curves are estimated. Altitude and velocity time histories are presented in figure 8 and Mach number and dynamic pressure variations are shown in figure 9. Velocity data between mortar fire and $t = 13.0$ seconds were determined by using accelerometers onboard the payload in conjunction with wind data. Figure 10 presents the velocity, Mach number, and dynamic pressure histories during the prime data period.

PARACHUTE PERFORMANCE

The primary objective of the flight test was to determine inflation, drag, and stability characteristics for the 64.7-foot (19.7-meter) diameter disk-gap-band parachute. For convenience, each property is discussed separately. A 16-millimeter motion-picture supplement showing the parachute inflation is available on loan. A request card for the film can be found at the back of this document.

Inflation Characteristics

The inflation sequence was initiated by the mortar firing the packed parachute rearward from the payload. Mortar fire (deployment) occurred at a Mach number of 1.59 and a dynamic pressure of 11.6 psf (555 N/m^2). The suspension lines strung out until line stretch, at which time the canopy began to emerge from the bag. After stripping off the canopy, the parachute bag continued rearward while the parachute inflated to a full condition. During the inflation process, sufficient drag was developed to pull the payload from the aeroshell. After full inflation, the canopy partially collapsed and then reinflated to a stable condition. During the reinflation process the parachute bag collided with the disk part of the parachute canopy and tore through two of the panels. The collision occurred because the high drag force developed by the inflated parachute caused the parachute to decelerate at a much higher rate than the parachute bag.

Times for significant events during parachute inflation were as follows:

Event	Onboard time, sec	Time from mortar fire, sec
Mortar fire	7.80	0
Line stretch	8.44	0.64
Estimated bag strip	8.87	1.07
Payload separation	9.39	1.59
Full inflation	9.40	1.60
Parachute bag collision	9.80	2.00
Stable inflation	10.80	3.00

Photographs taken by the high-speed (≈350-frame-per-second) payload camera are presented in figure 11. Figure 11(a) shows three frames during the initial inflation sequence. Figure 11(b) shows full inflation followed by partial collapse. Reinflation and growth to stable inflation are shown in figures 11(c) and 11(d). It is believed that this partial collapse and reinflation process represents the response of the flexible parachute and suspension-line system to the rapidly applied initial load.

Inflation loads were measured by the two longitudinal accelerometers and the tensiometer and are presented in figures 12 and 13. Figure 14 shows in detail the accelerations recorded between mortar fire and the stripping of the bag off the canopy. Growth of the parachute canopy projected area during inflation is depicted in figure 15. Shown is the ratio of the projected area at time t to the projected area at stable inflation ($t = 10.8$ seconds). Full inflation occurred at $t = 9.4$ seconds and partial collapse at about $t = 9.6$ seconds. The mean of the oscillation shows a gradual growth in parachute projected area with time; this gradual growth possibly indicates canopy shape change as the Mach number and dynamic pressure decrease. By using camera 3 film, the parachute diameter was determined to be about 54 percent D_o at stable inflation and 65 percent D_o during descent.

Drag Characteristics

Drag characteristics for the parachute-payload system during deceleration through the Mach number range (prior to apogee) were determined by using accelerometer and tensiometer data. From accelerometer results

$$C_{D,o} = \frac{-W_{total} a_l}{q_\infty S_o}$$

and using tensiometer data

$$C_{D,o} = \frac{W_{total}}{W_{payload}} \frac{T}{q_\infty S_o}$$

The weight of the total system was 557 pounds mass (253 kg) and the weight of the payload (including bridle but not tensiometer) was 470.0 pounds mass (213.2 kg). Figure 16 shows the variation of $C_{D,o}$ with Mach number by using both accelerometer and tensiometer data. In the region after stable inflation ($M = 0.85$ to $M = 0.4$), the average value of $C_{D,o}$ is estimated to be about 0.55. Fluctuations in canopy shape possibly cause the large $C_{D,o}$ oscillations prior to stable inflation. Estimated uncertainty for the drag coefficient is ±0.04 near the high Mach number region ($M = 0.85$) of stable inflation. The uncertainty is based on a first-order analysis with 3-percent velocity error, 3-percent density error, and 1 percent accelerometer or tensiometer error being

assumed. In the low Mach number region (M = 0.4), the estimated uncertainty is ±0.07 because of a possible 12-percent error in velocity.

Values for the "effective" drag coefficient $(C_{D,o})_{eff}$ based on vertical-descent velocity were calculated by using the following equation:

$$(C_{D,o})_{eff} = \frac{2W_{total}}{\rho_\infty S_o \dot{Z}_E^2}$$

Variation of $(C_{D,o})_{eff}$ with altitude is shown in figure 17. The amount of uncertainty indicated is based on 3-percent errors in both descent velocity and density. No consideration was given to possible vertical wind draft conditions which may have influenced the data.

Stability Characteristics

Stability characteristics of the descending parachute system were determined from both trajectory and onboard camera data. Photographs from camera 2 (fig. 2) viewing the horizon were analyzed by using the methods of reference 7 extended to the conditions of this test. Attitude angles of the payload relative to the local horizon were obtained. The body-axis Euler angle system shown in figure 18 was used for ease of data reduction. The angle ψ is the azimuth of the body X-axis and θ and ϕ are measures of the pitching and yawing motions. The resultant angle δ is the total pitch-yaw displacement of the longitudinal axis from the local vertical. Time histories of θ, ϕ, and δ depicting the pitching and yawing motions are shown in figure 19. These data are estimated to be accurate within 3^o. Observation of the camera 3 film indicates that relative motion in pitch and yaw between the payload and the parachute had a maximum amplitude of less than 2^o after a flight time of 35 seconds. Thus, the angular time histories shown in figure 19 are essentially those of the parachute. Figure 20 shows δ as a function of altitude. The sharp variations of δ with altitude are possibly caused by the wind-shear conditions prevalent during parachute descent. The δ histories shown in both figures 19 and 20 indicate an average or trim value of the parachute-payload system of approximately 5^o throughout most of the data period. Since the pitching and yawing amplitude about trim were relatively small after stable inflation, the parachute stability characteristics are considered to be good.

PARACHUTE STRUCTURAL DAMAGE

After recovery the disk-gap-band parachute was inspected for structural damage. The only major damage to occur during the test was two torn panels in the parachute disk

caused by the parachute bag passing through the canopy after inflation. A photograph of the damaged parachute taken by camera 3 during descent is shown in figure 21. Figure 22 is a sketch showing the approximate size and shape of the tear. As noted, the tear extended across two panels, and the cross-seam reinforcing tape pulled out of the main seam. By considering the area loss caused by the two torn panels, the geometric porosity of the parachute increased from 12.35 percent to 12.80 percent. Minor damage included a 1-inch (2.54-cm) tear in the band, probably caused by brush in the impact area, and some very small stretch marks in a panel near the canopy vent, which could have occurred during fabrication. It is believed that parachute performance was little affected by any of the damage.

CONCLUDING REMARKS

Inflation, drag, and stability characteristics of a 64.7-foot nominal-diameter (19.7-meter) disk-gap-band parachute were obtained from the second flight of the balloon-launched series of the Planetary Entry Parachute Program. Deployment occurred at a Mach number of 1.59 and a dynamic pressure of 11.6 psf (555 N/m^2). After ejection from the payload, the parachute rapidly inflated to a full condition, partially collapsed, and reinflated to a stable condition. During the reinflation process, the bag in which the parachute was packed prior to deployment collided with the canopy. Two disk panels, representing less than 0.5 percent of the total surface area, were torn during the collision; however, this damage did not appear to have any effect on parachute performance. After stable inflation, the parachute developed a drag coefficient near 0.55 based on nominal surface area. During descent, the parachute-payload combination had an aerodynamic trim angle of about 5° and exhibited good stability characteristics.

Langley Research Center,
National Aeronautics and Space Administration,
Langley Station, Hampton, Va., December 15, 1967,
124-07-03-05-23.

REFERENCES

1. McFall, John C., Jr.; and Murrow, Harold N.: Parachute Testing at Altitudes Between 30 and 90 Kilometers. AIAA Aerodynamic Deceleration Systems Conference, Sept. 1966, pp. 116-121.

2. Preisser, John S.; Eckstrom, Clinton V.; and Murrow, Harold N.: Flight Test of a 31.2-Foot-Diameter Modified Ringsail Parachute Deployed at a Mach Number of 1.39 and a Dynamic Pressure of 11.0 Pounds per Square Foot. NASA TM X-1414, 1967.

3. Eckstrom, Clinton V.; and Preisser, John S.: Flight Test of a 30-Foot-Nominal-Diameter Disk-Gap-Band Parachute Deployed at a Mach Number of 1.56 and a Dynamic Pressure of 11.4 Pounds per Square Foot. NASA TM X-1451, 1967.

4. Eckstrom, Clinton V.; Murrow, Harold N.; and Preisser, John S.: Flight Test of a 40-Foot-Nominal-Diameter Modified Ringsail Parachute Deployed at a Mach Number of 1.64 and a Dynamic Pressure of 9.1 Pounds per Square Foot. NASA TM X-1484, 1967.

5. Whitlock, Charles H.; Bendura, Richard J.; and Coltrane, Lucille C.: Performance of a 26-Meter-Diameter Ringsail Parachute in a Simulated Martian Environment. NASA TM X-1356, 1967.

6. Darnell, Wayne L.; Henning, Allen B.; and Lundstrom, Reginald R.: Flight Test of a 15-Foot-Diameter (4.6-Meter) 120^{o} Conical Spacecraft Simulating Parachute Deployment in a Mars Atmosphere. NASA TN D-4266, 1967.

7. Anon.: Manual of Photogrammetry. Sec. ed., American Soc. Photogrammetry, c.1952.

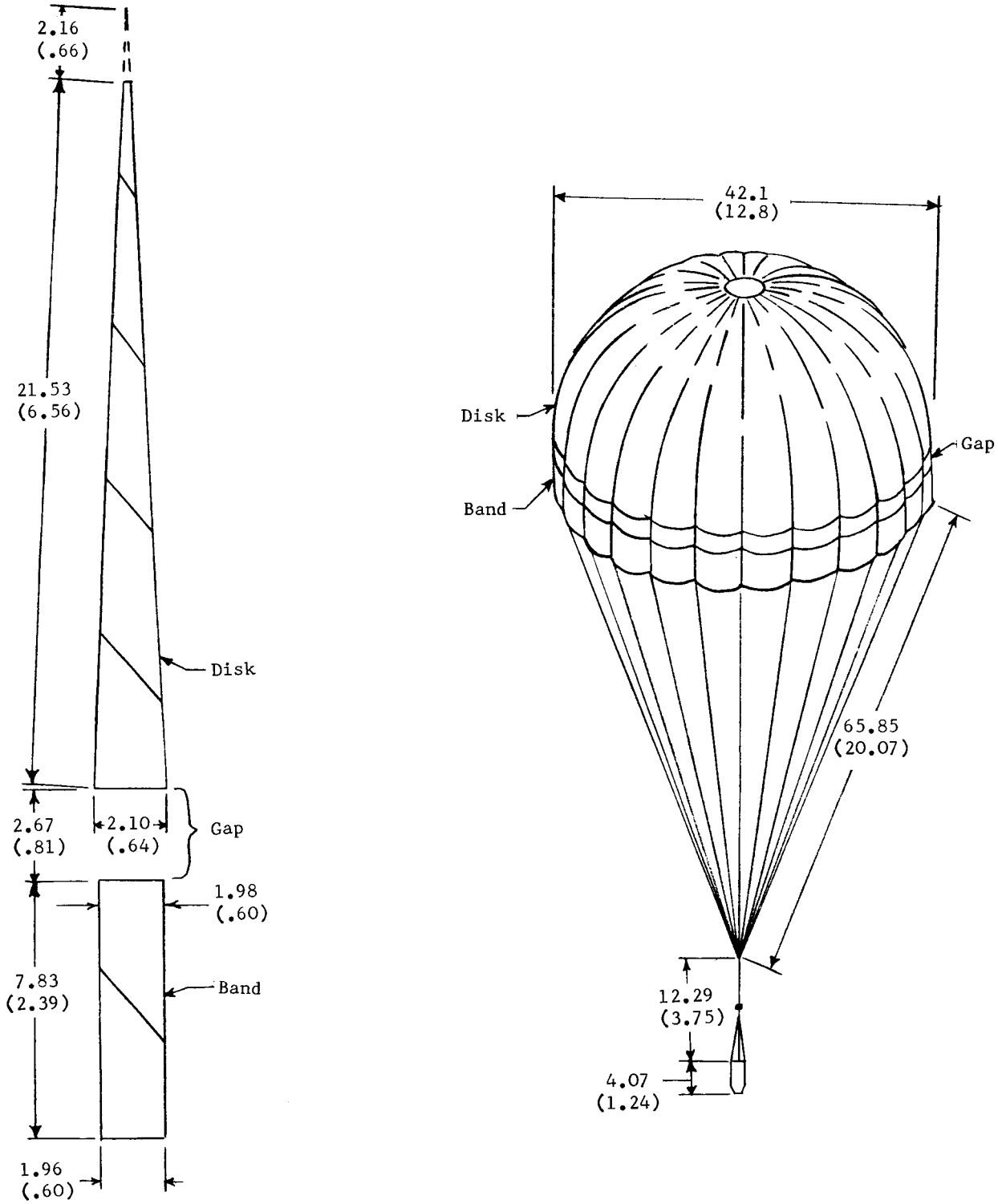

Figure 1.- Sketch showing a typical gore and the parachute-payload configuration. Gore dimensions are an average of the actual measurements of all 72 gores. Dimensions shown are in feet (meters).

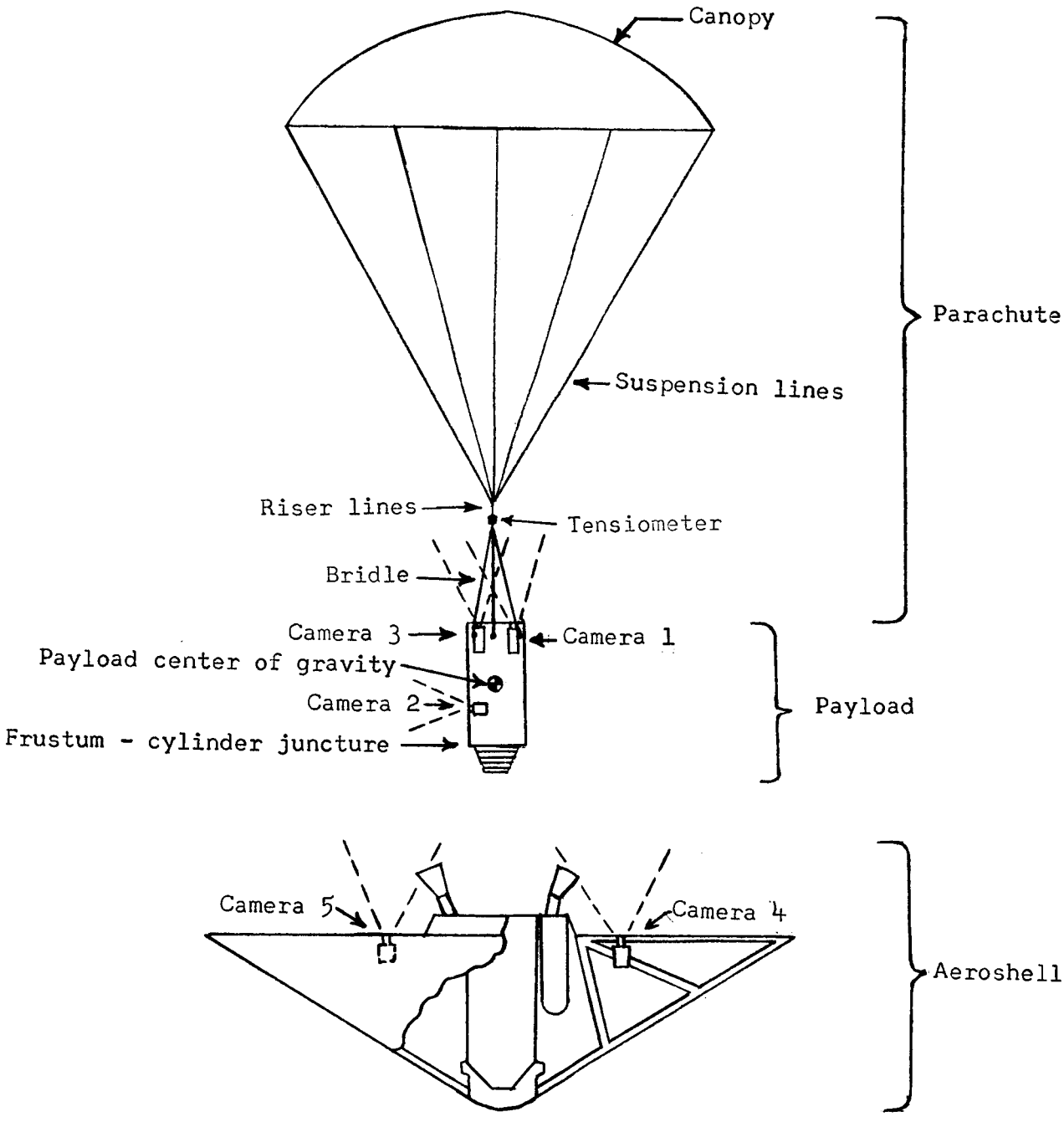

Figure 2.- Sketch of spacecraft components.

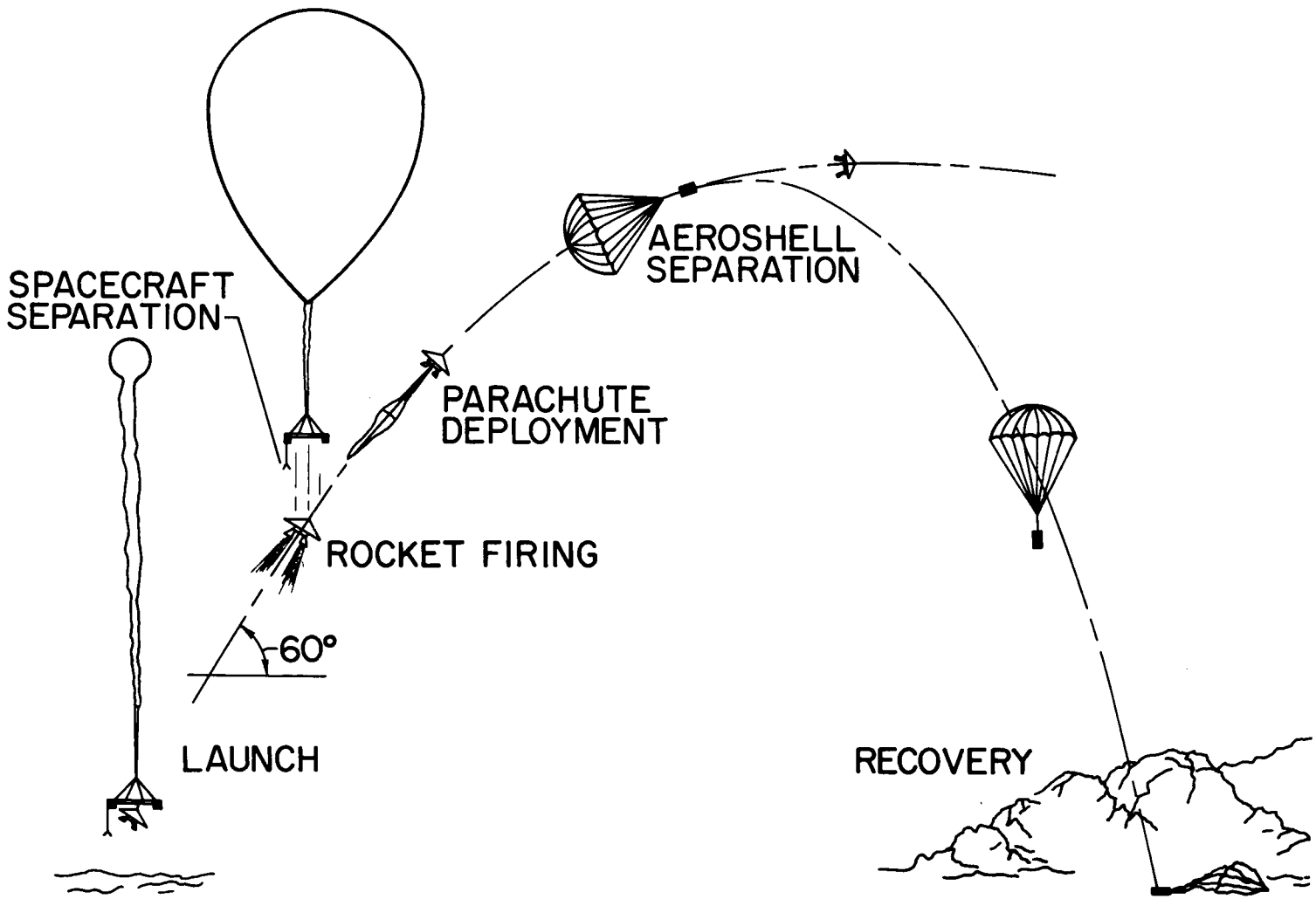

Figure 3.- Mission profile.

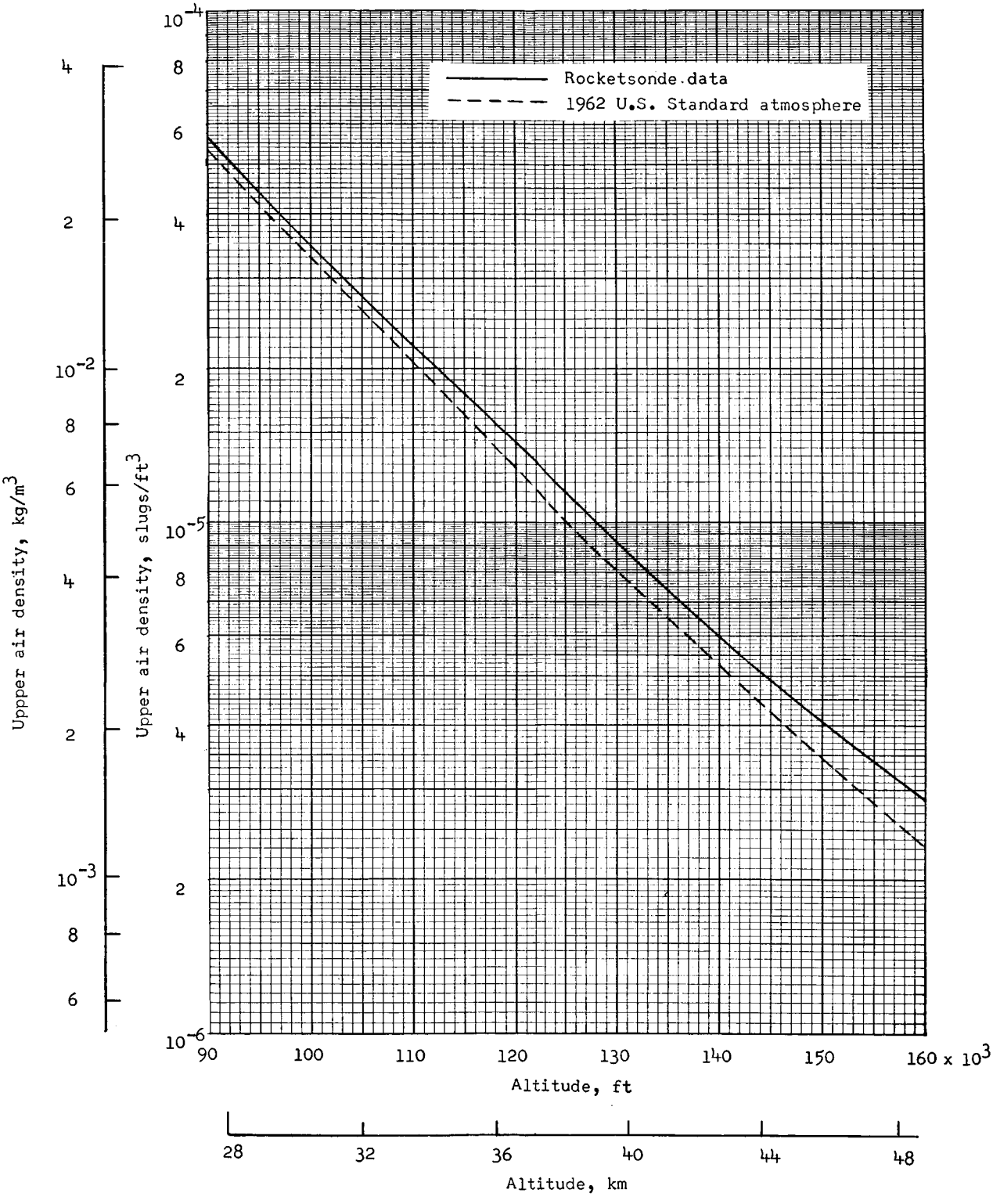

Figure 4.- Atmospheric density.

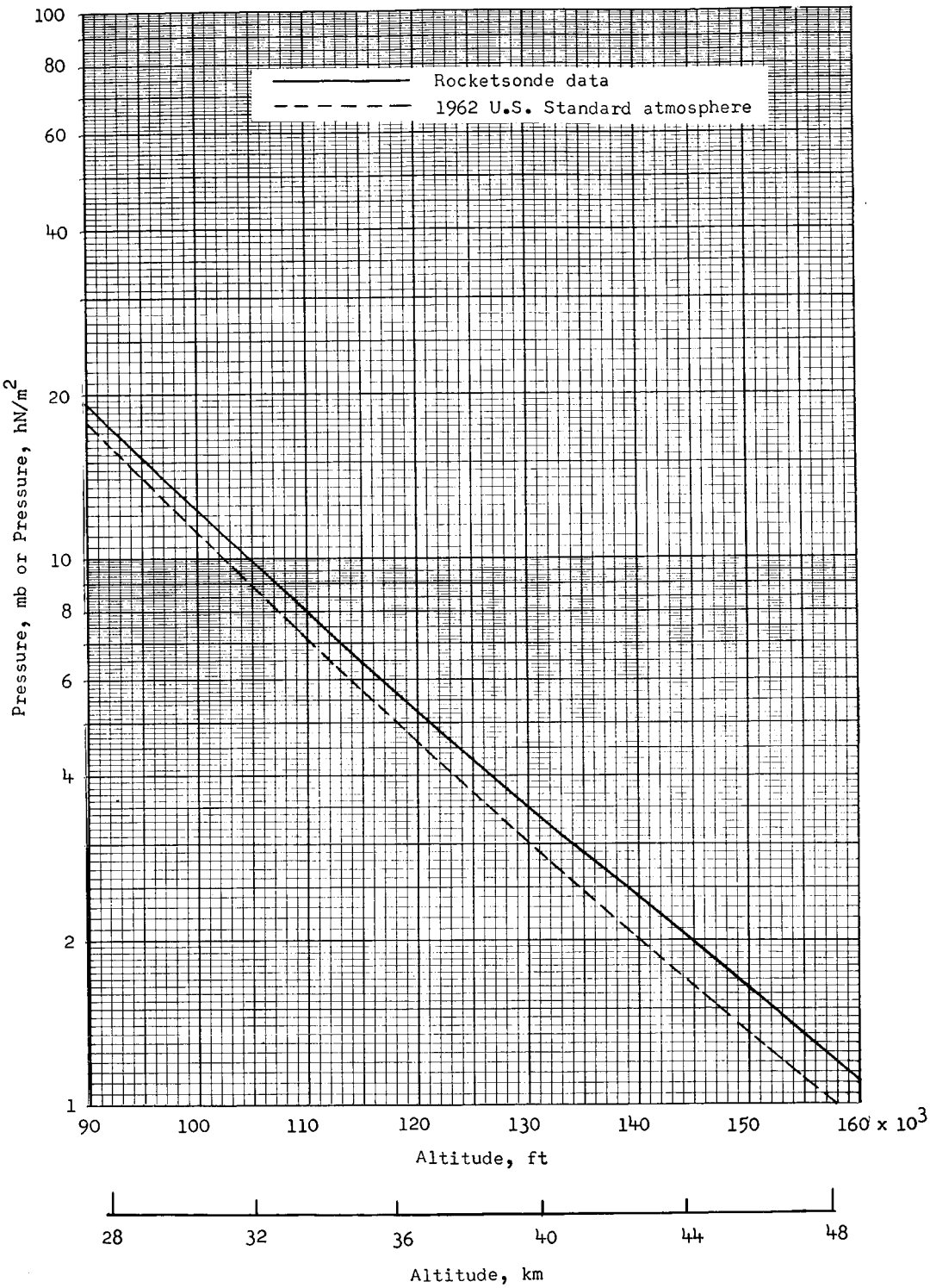

Figure 5.- Atmospheric pressure.

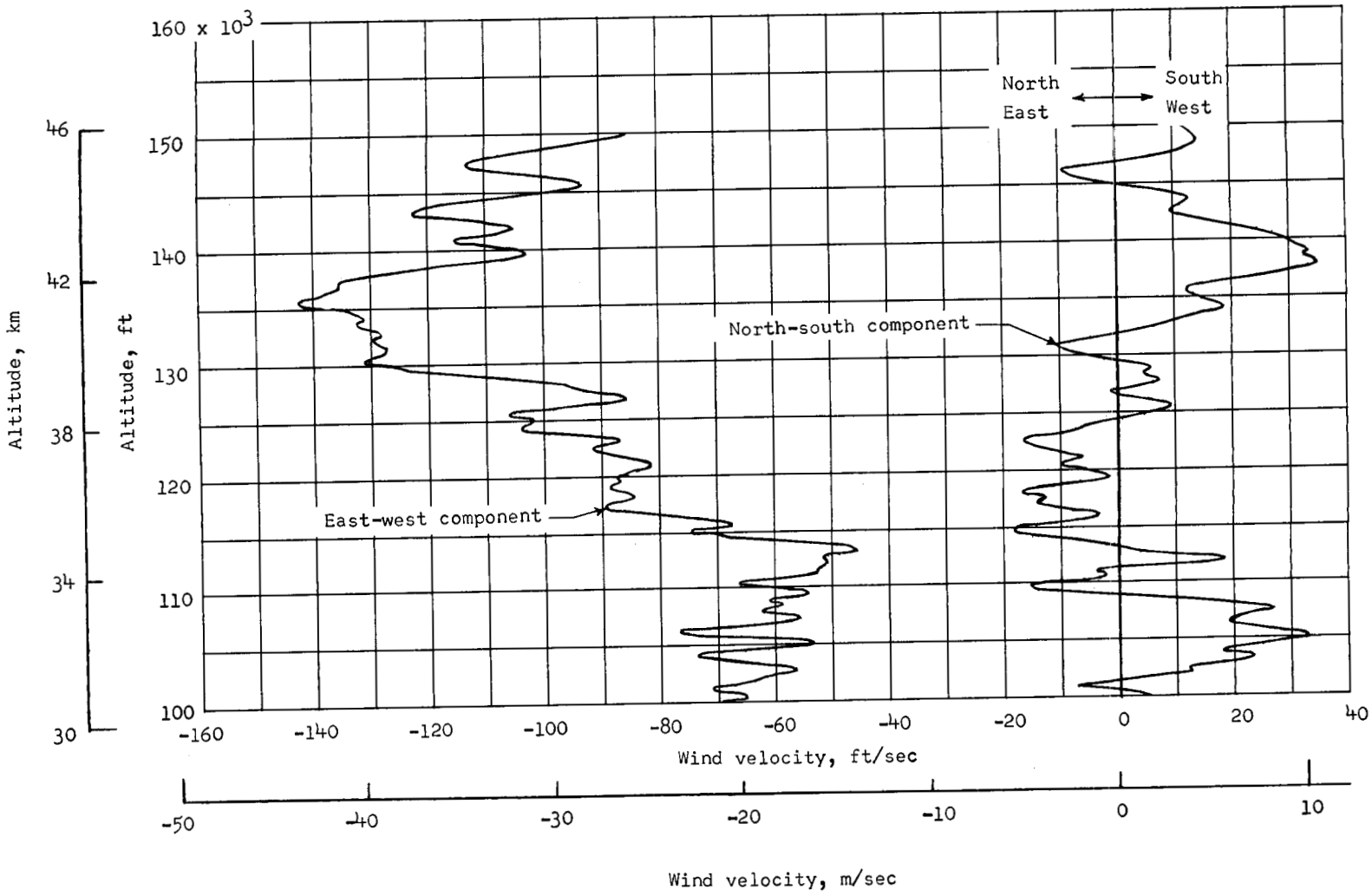

Figure 6.- Wind-velocity profile in east-west and north-south components.

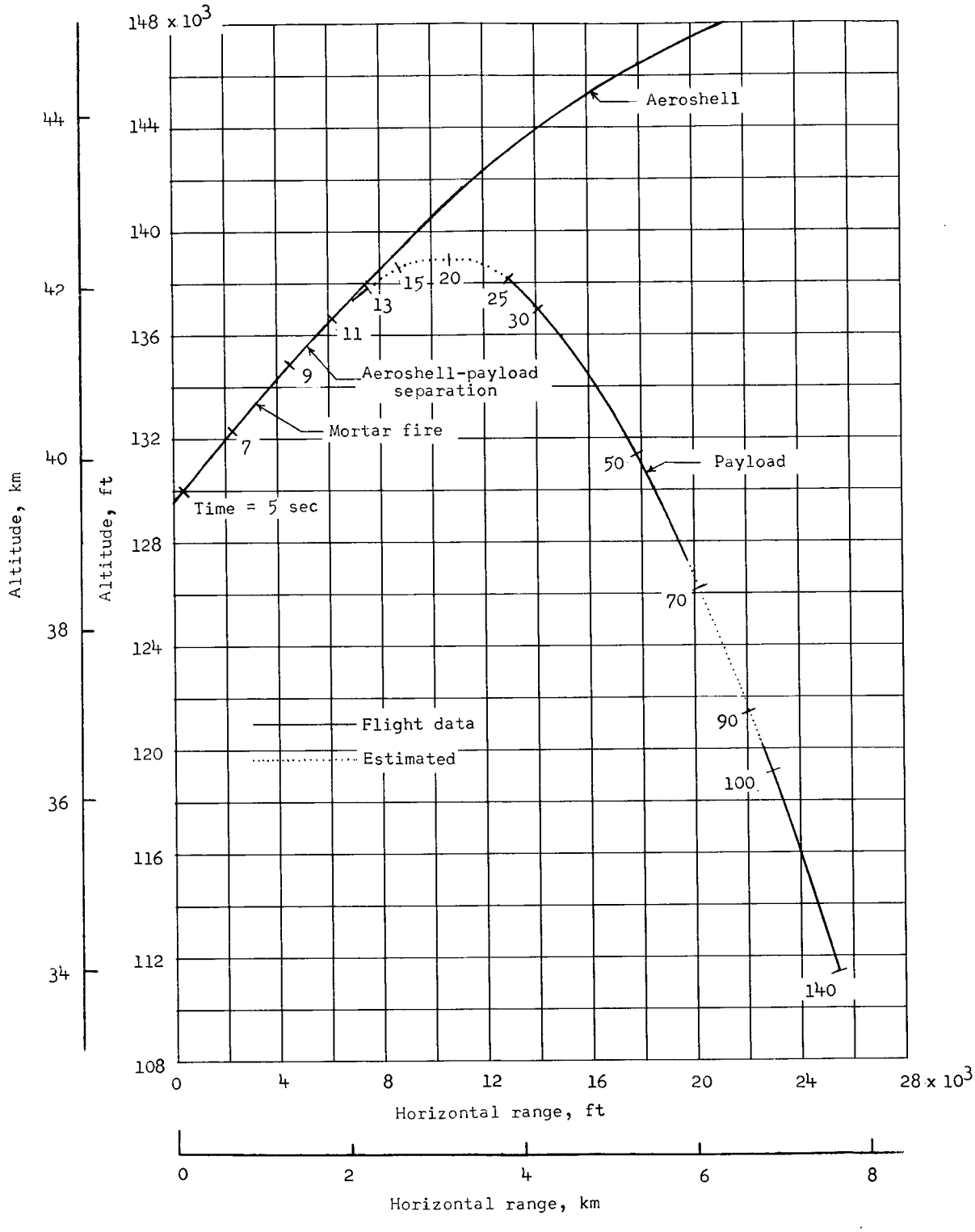

Figure 7.- Variation of altitude with horizontal range.

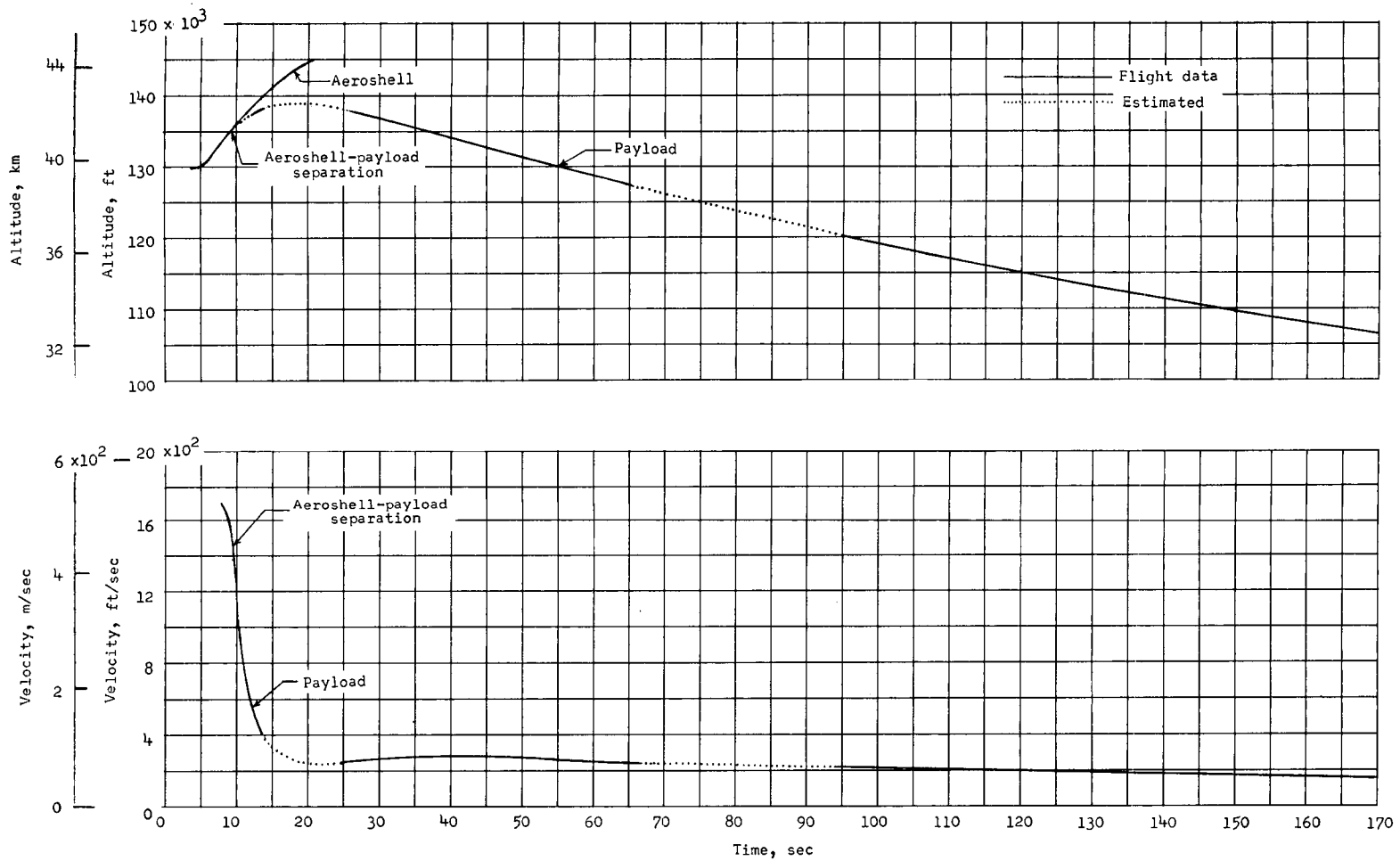

Figure 8.- Altitude and velocity time histories.

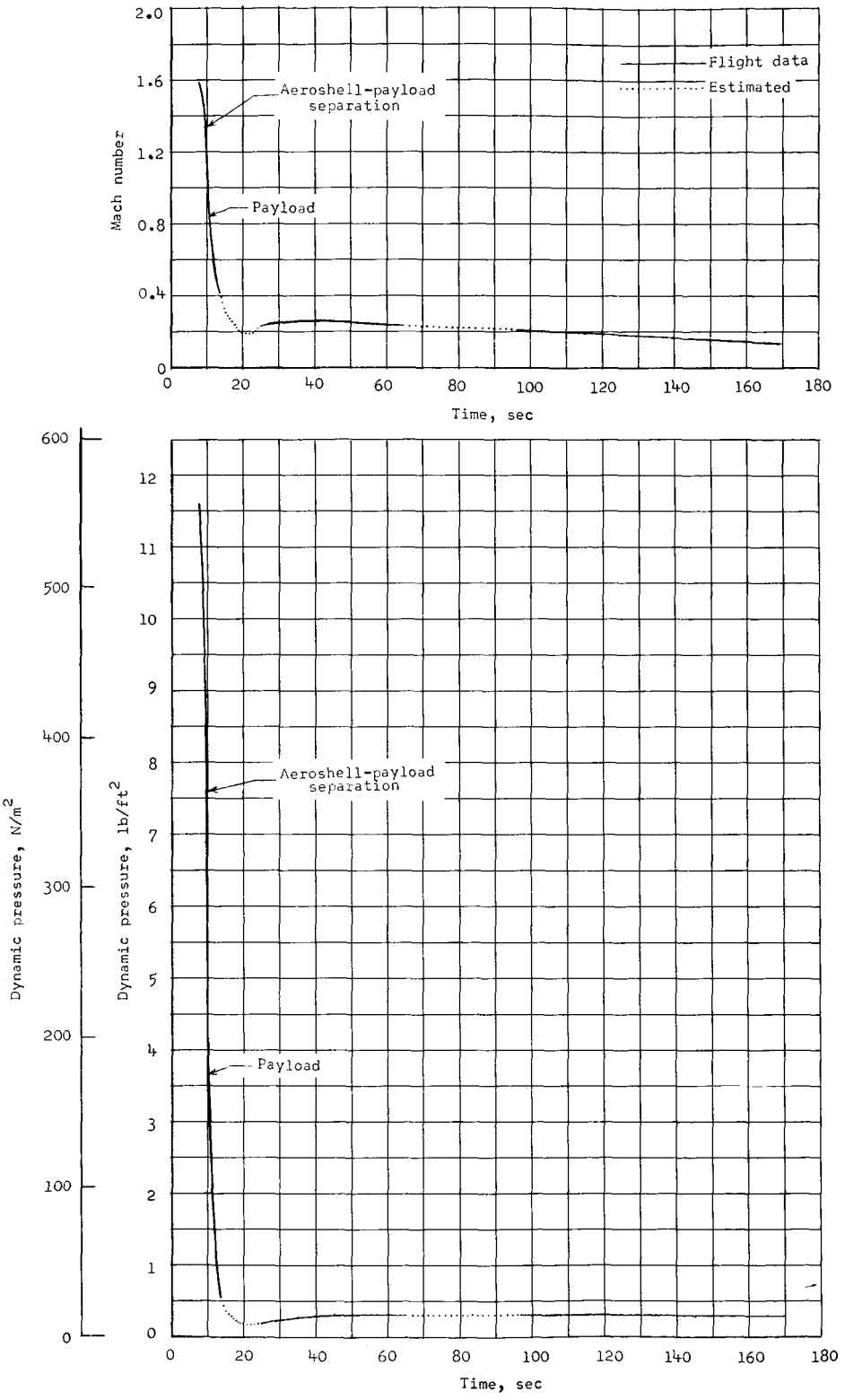

Figure 9.- Mach number and dynamic pressure time histories.

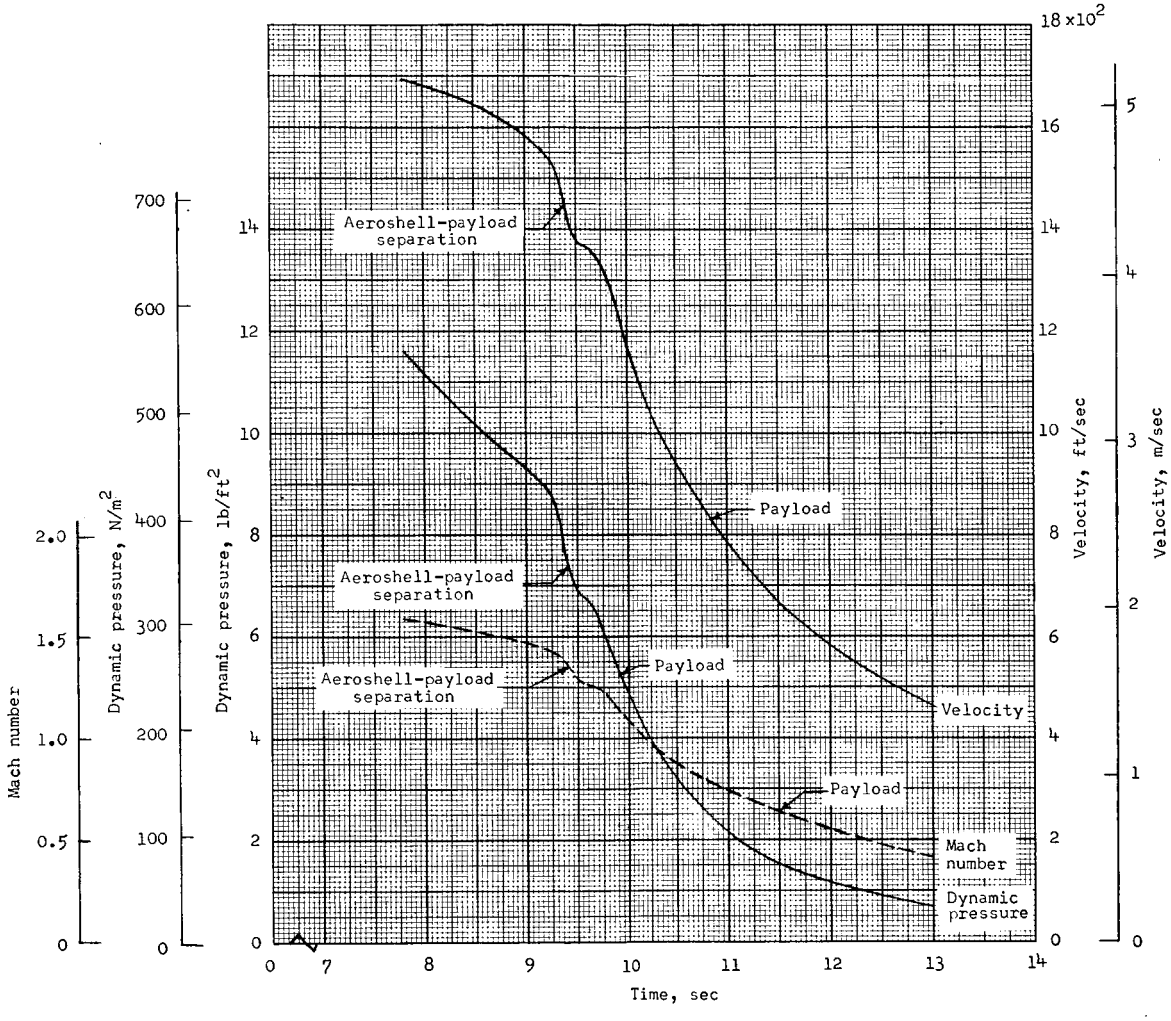

Figure 10.- Velocity, dynamic pressure, and Mach number time histories during parachute deployment.

Time = 8.99 seconds

Time = 9.19 seconds

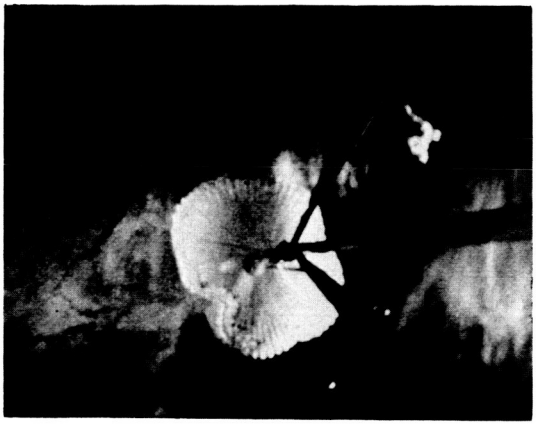

Time = 9.32 seconds

(a) Initial inflation.

L-67-8730

Figure 11.- Onboard camera photographs.

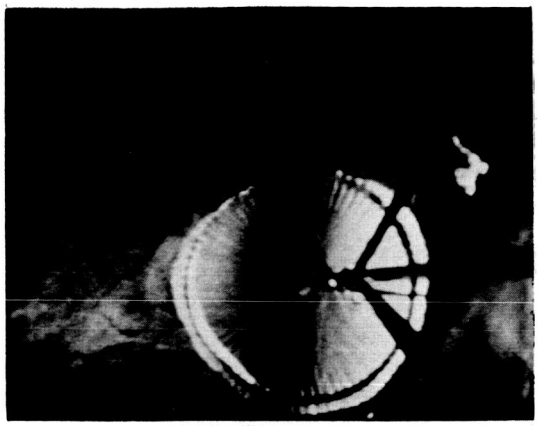

Time = 9.39 seconds

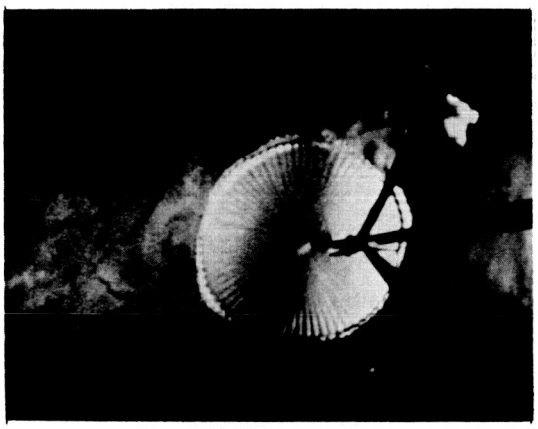

Time = 9.45 seconds

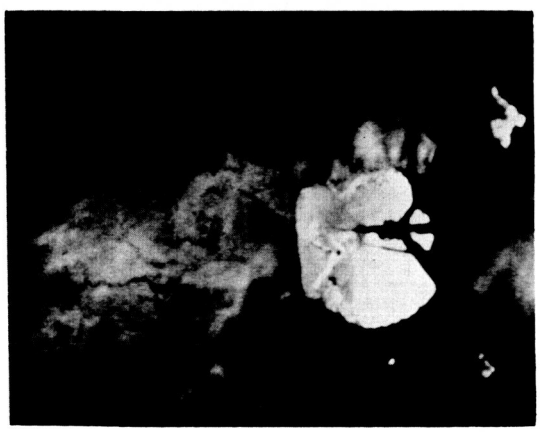

Time = 9.58 seconds

(b) Full inflation and collapse.

L-67-8731

Figure 11.- Continued.

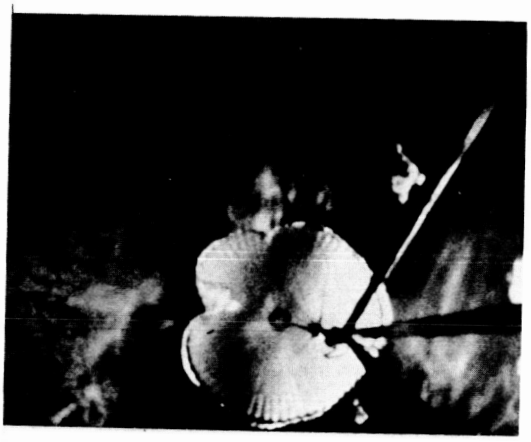

Time = 9.74 seconds

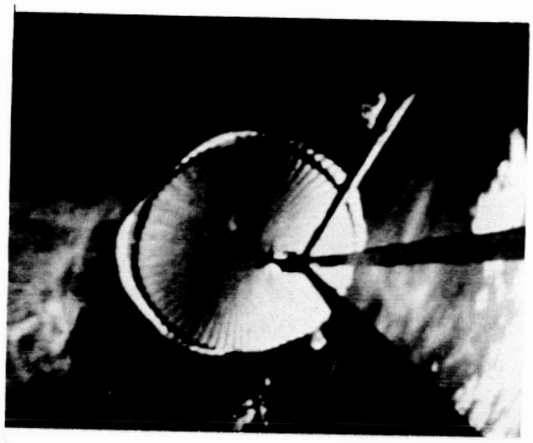

Time = 9.80 seconds

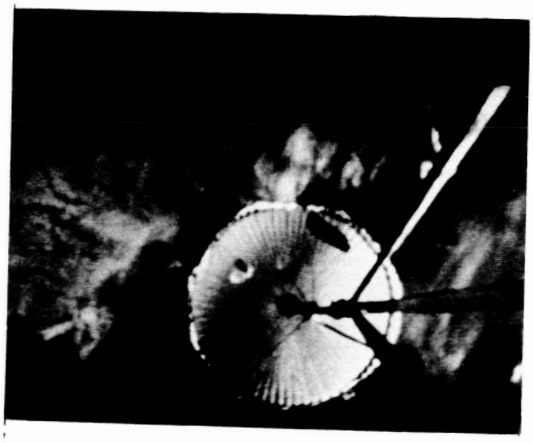

Time = 9.94 seconds

(c) Reinflation.

L-67-8732

Figure 11.- Continued.

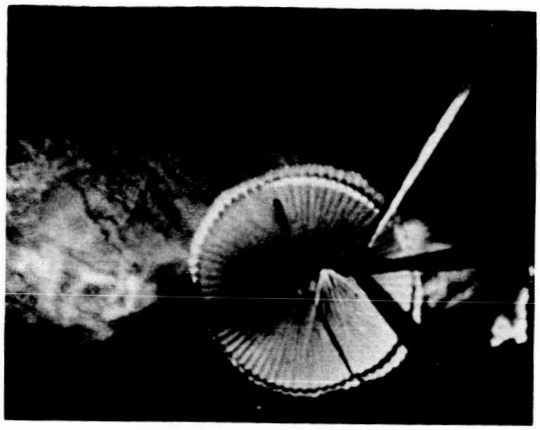

Time = 10.39 seconds

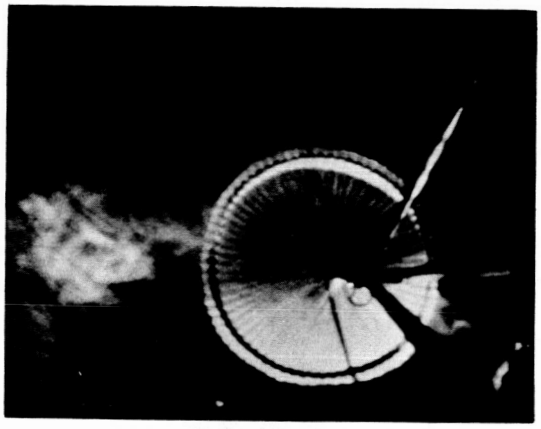

Time = 10.99 seconds

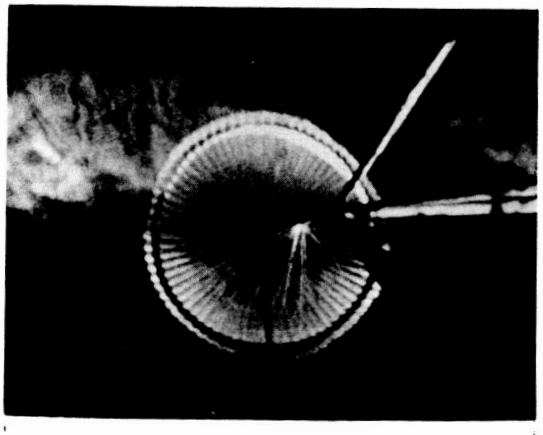

Time = 11.59 seconds

(d) Growth to stable inflation.

L-67-8733

Figure 11.- Concluded.

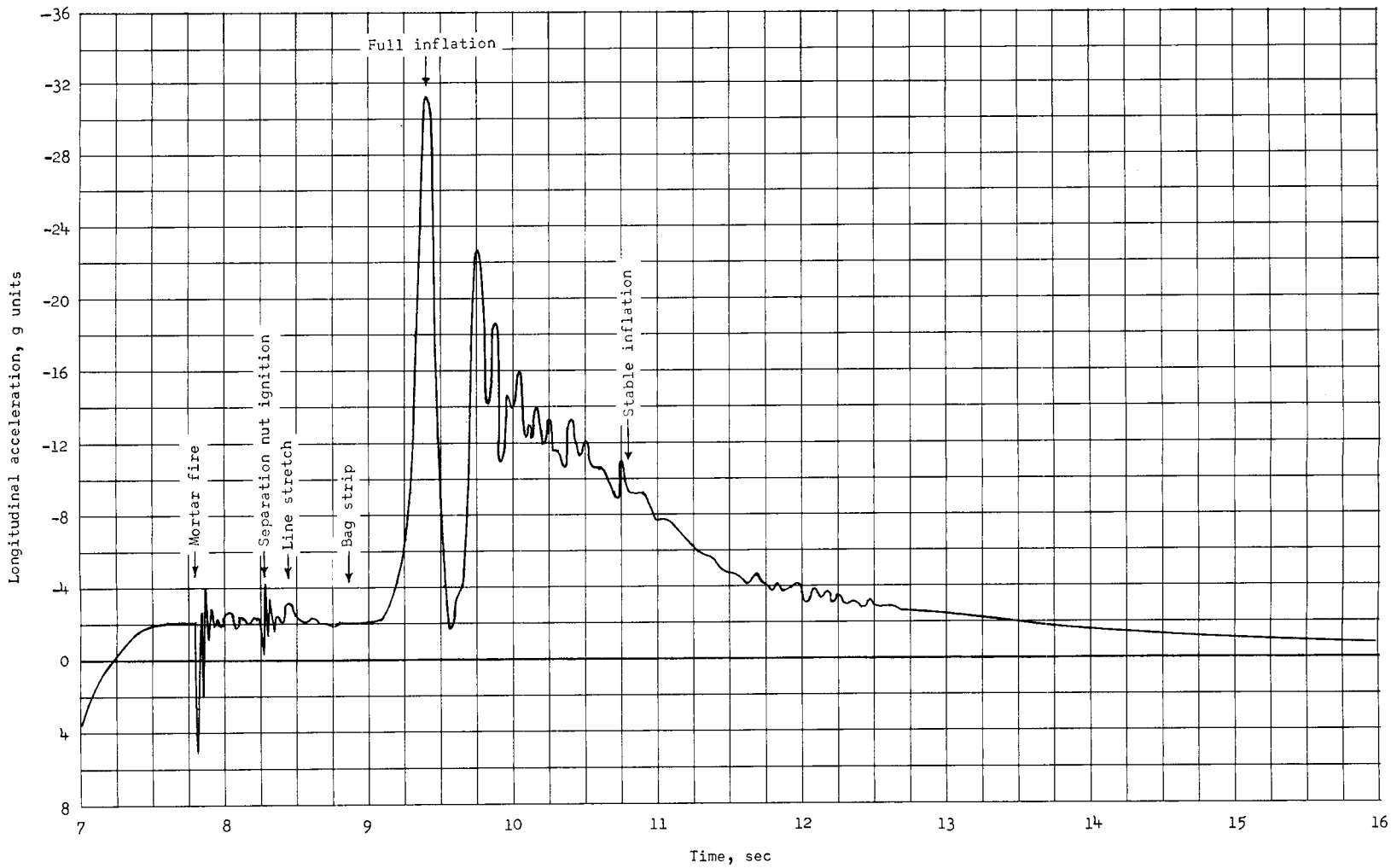

Figure 12.- Longitudinal acceleration time history.

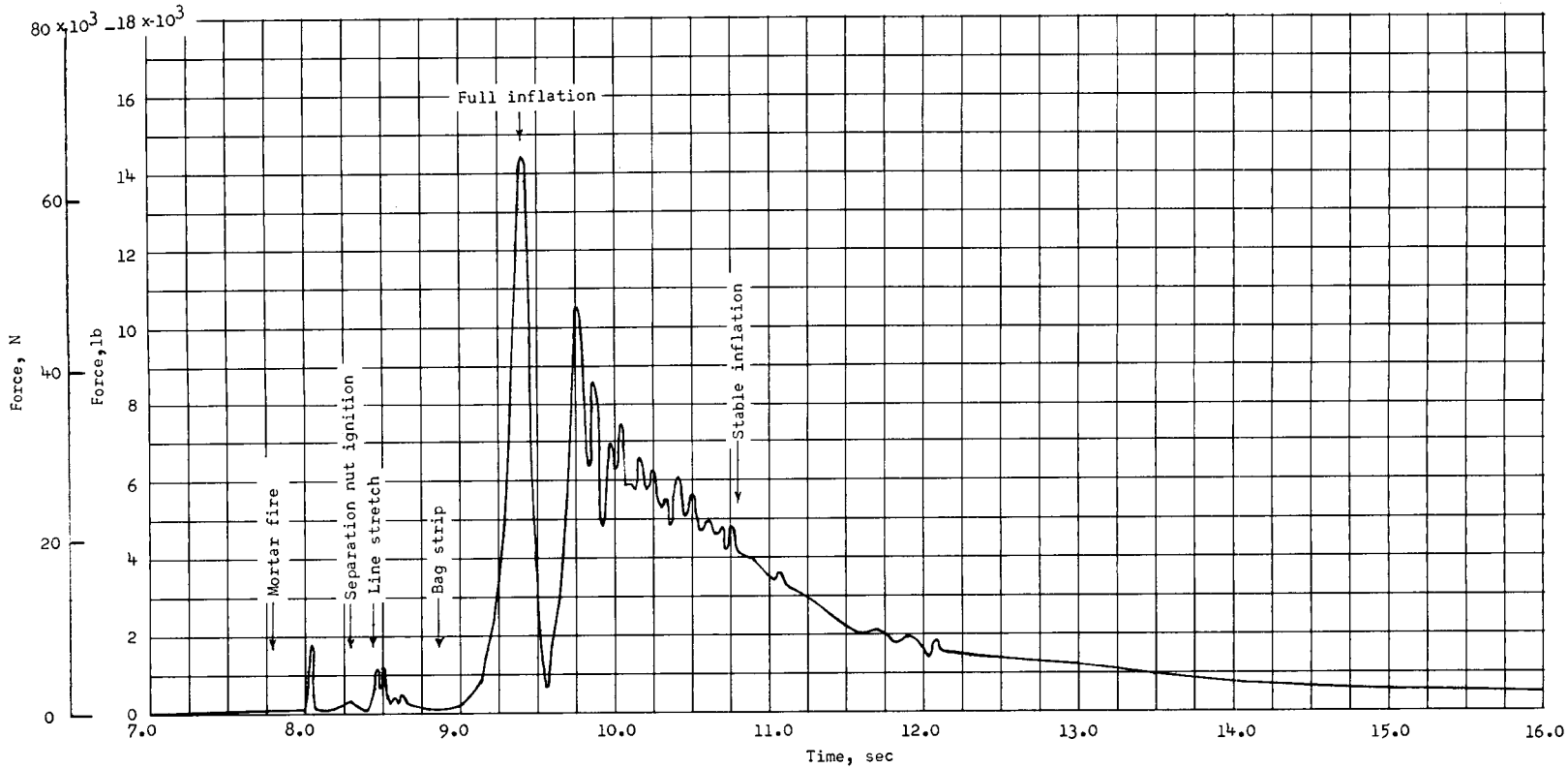

Figure 13.- Tensiometer load time history.

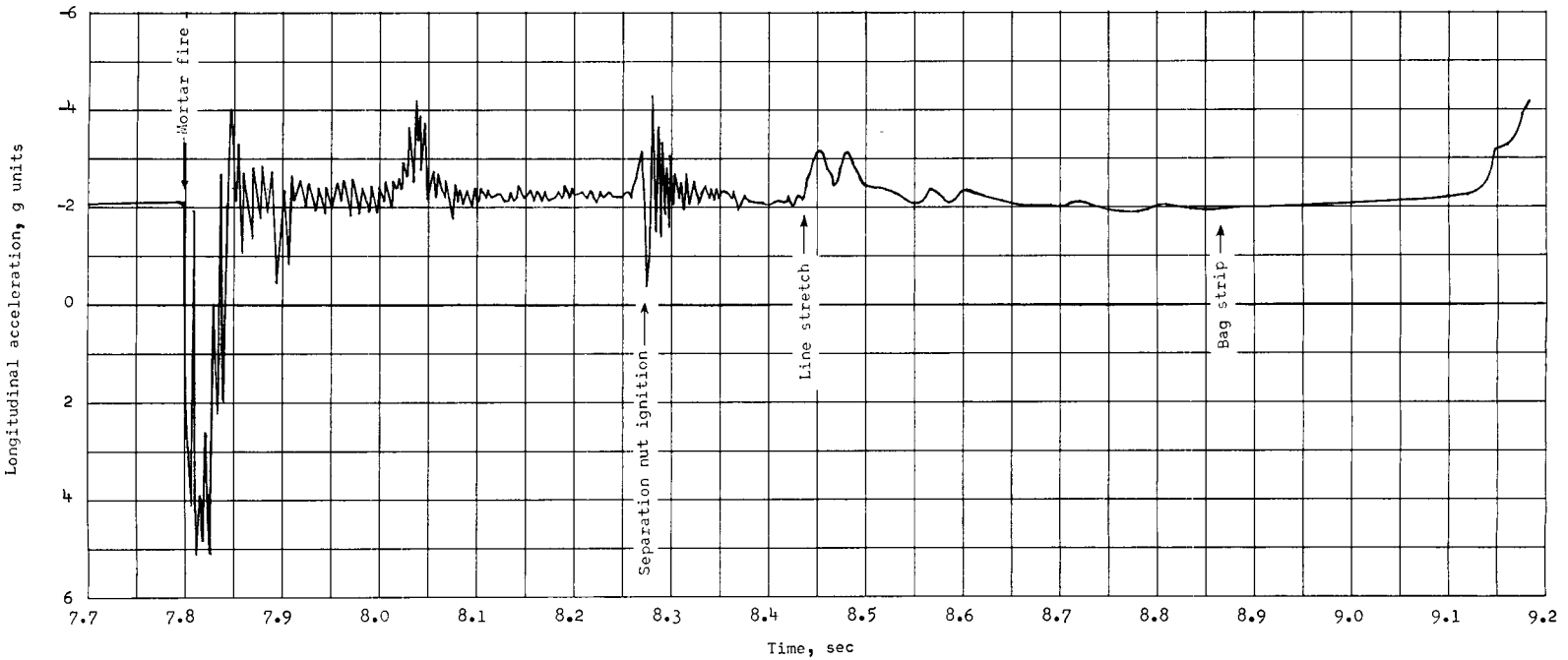

Figure 14.- Longitudinal acceleration time history during parachute deployment.

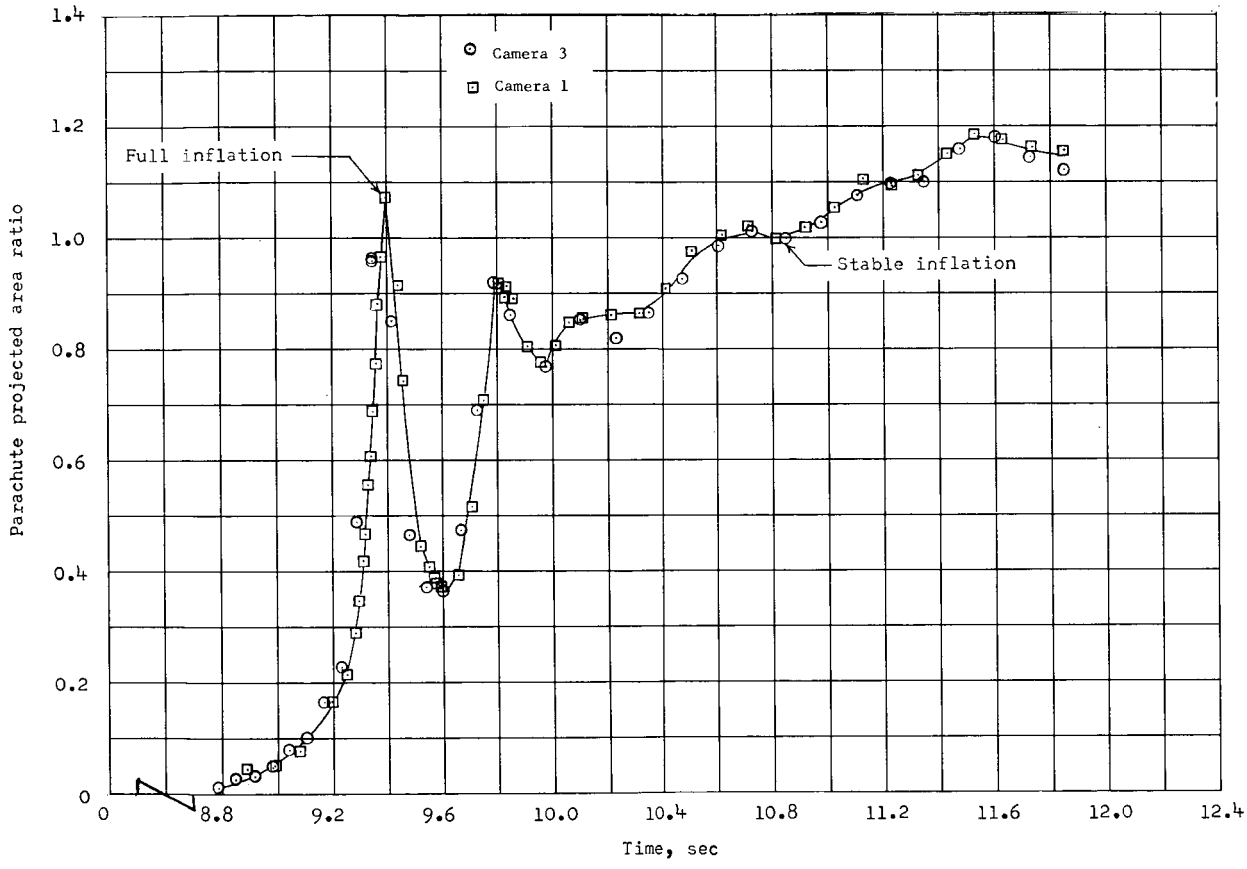

Figure 15.- Parachute projected-area-ratio time history.

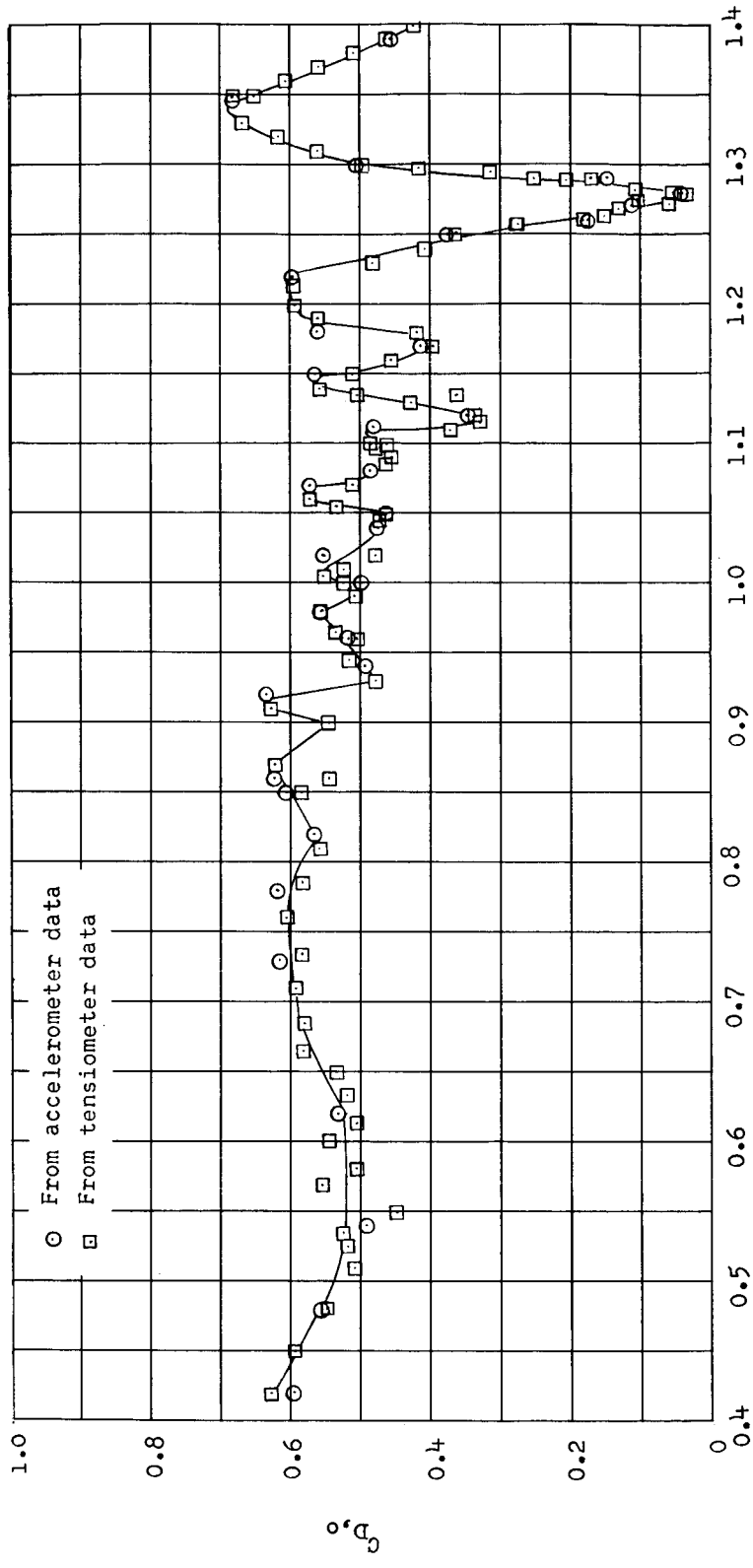

Figure 16.- Variation of parachute drag coefficient with Mach number.

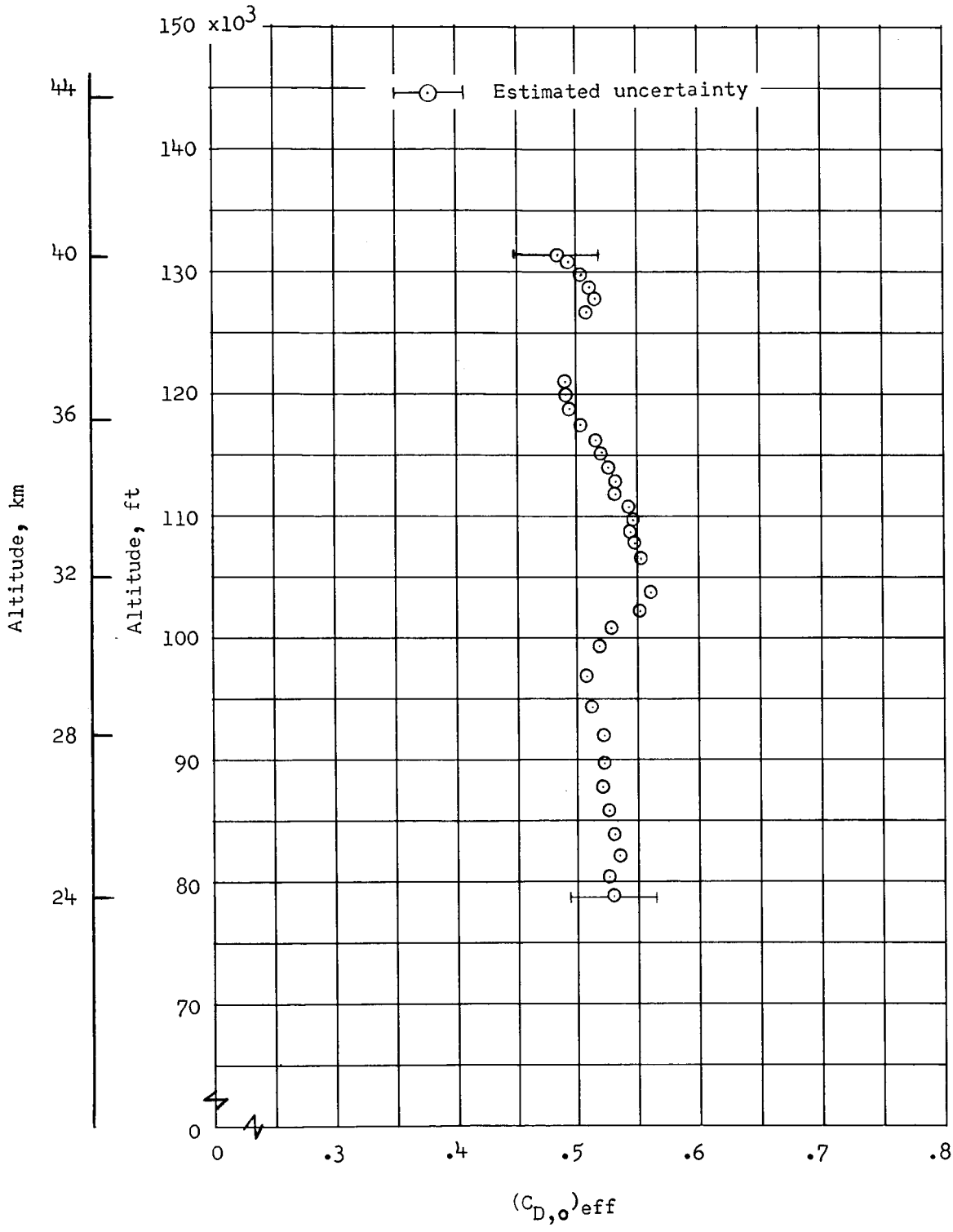

Figure 17.- Variation of effective drag coefficient with altitude.

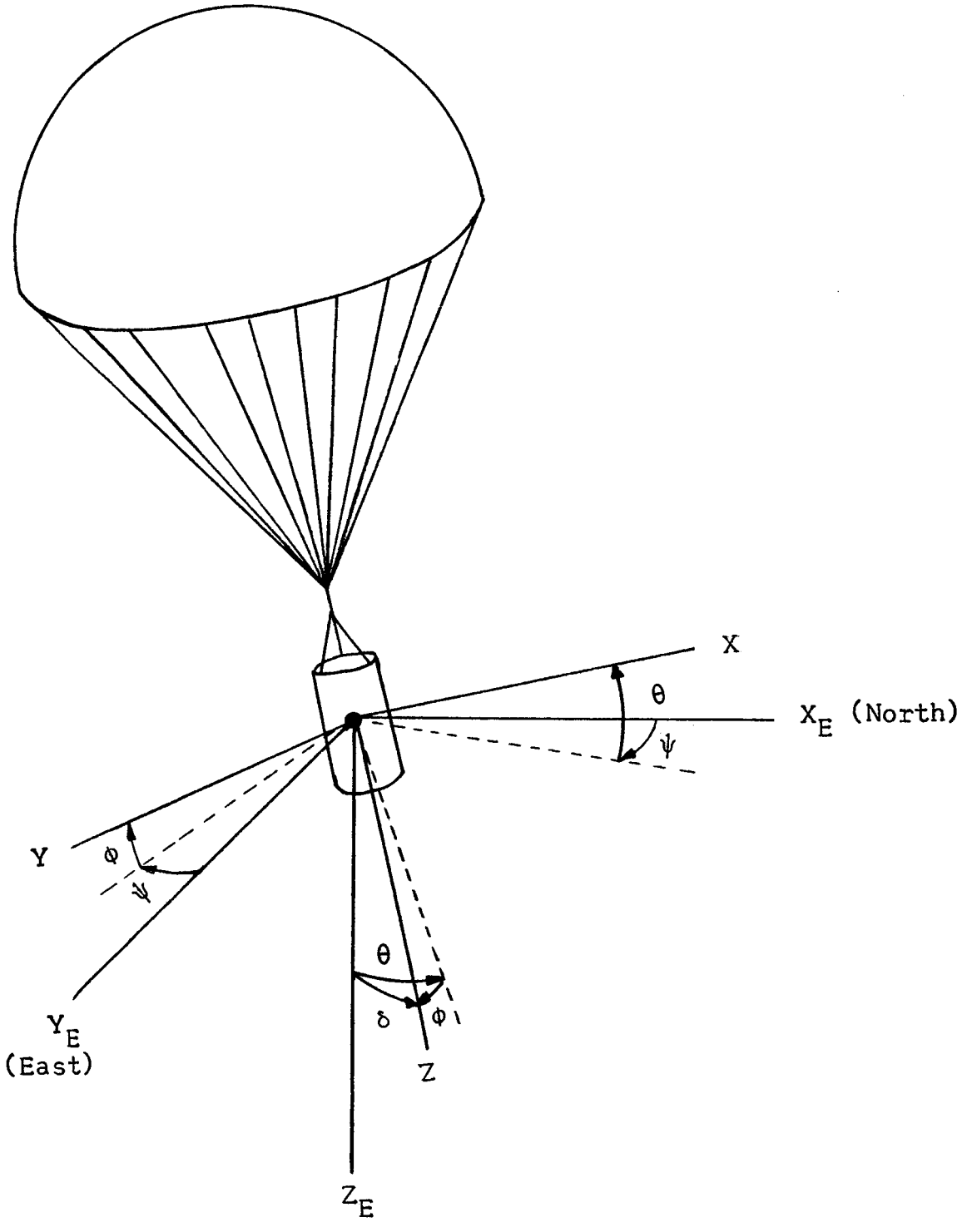

Figure 18.- Body-axis system orientation.

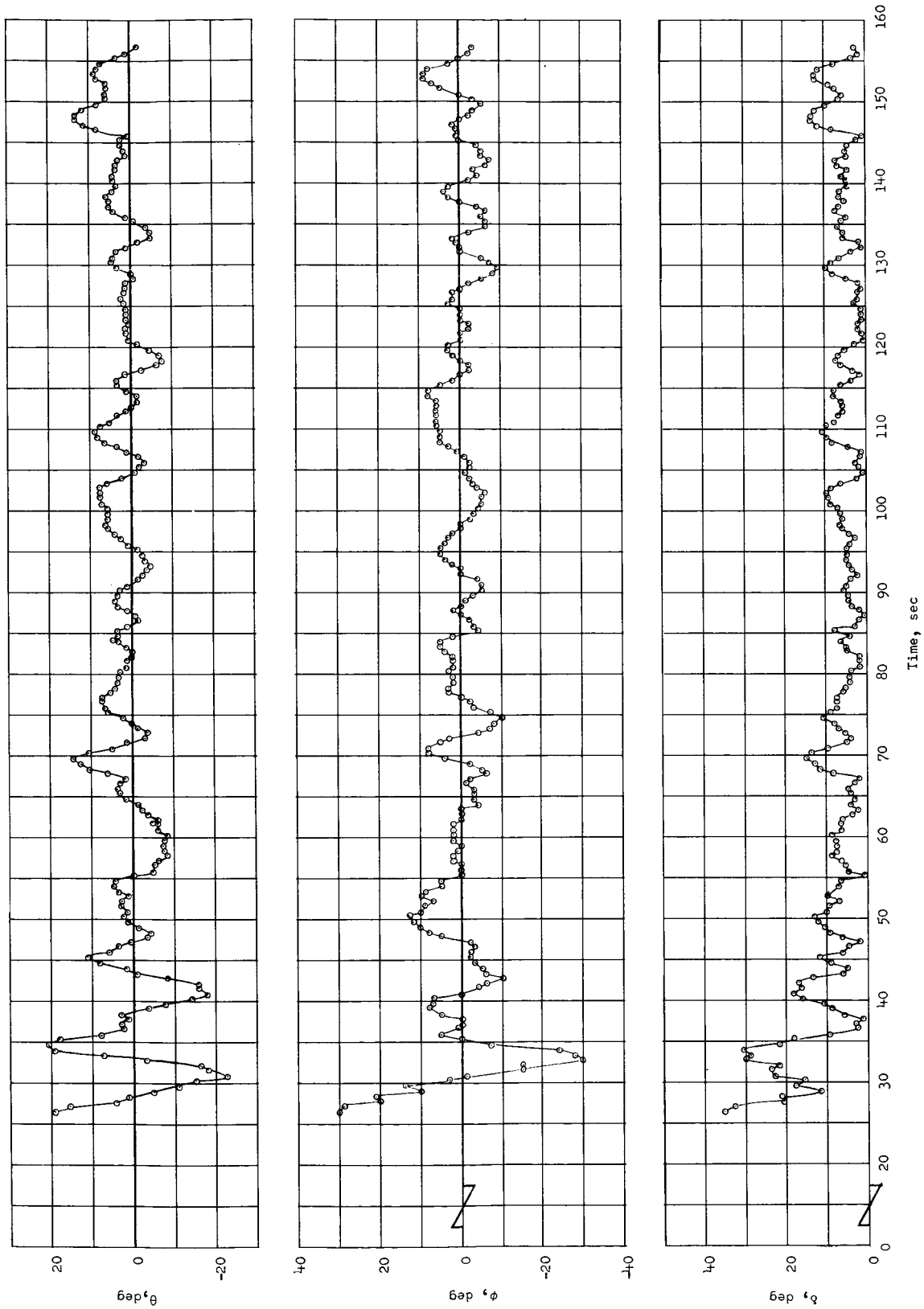

Figure 19.- Time histories of θ, Φ, and δ.

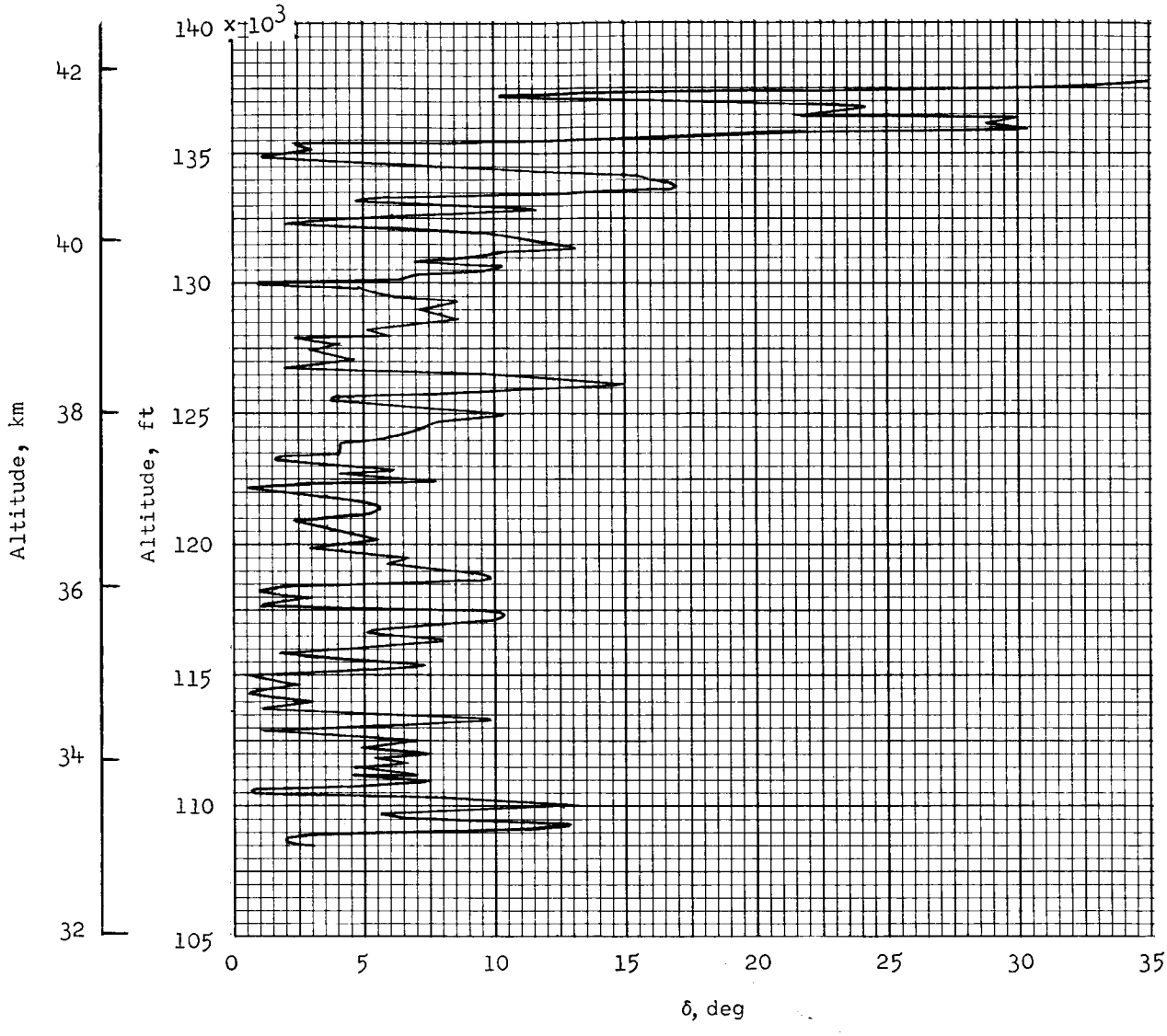

Figure 20.- Total pitch-yaw displacement as a function of altitude.

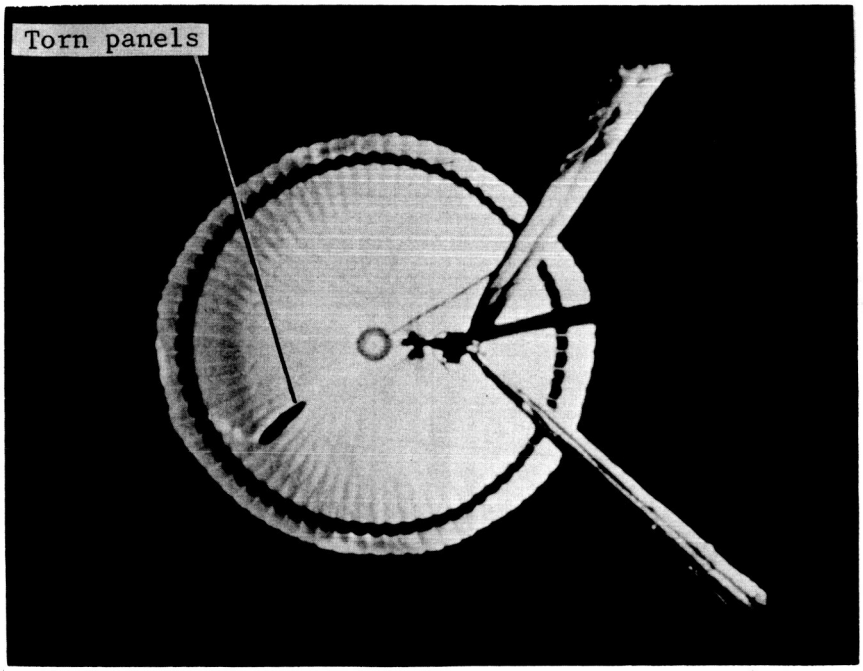

Figure 21.- Photograph of damaged parachute. t = 94.91 seconds. L-67-8734

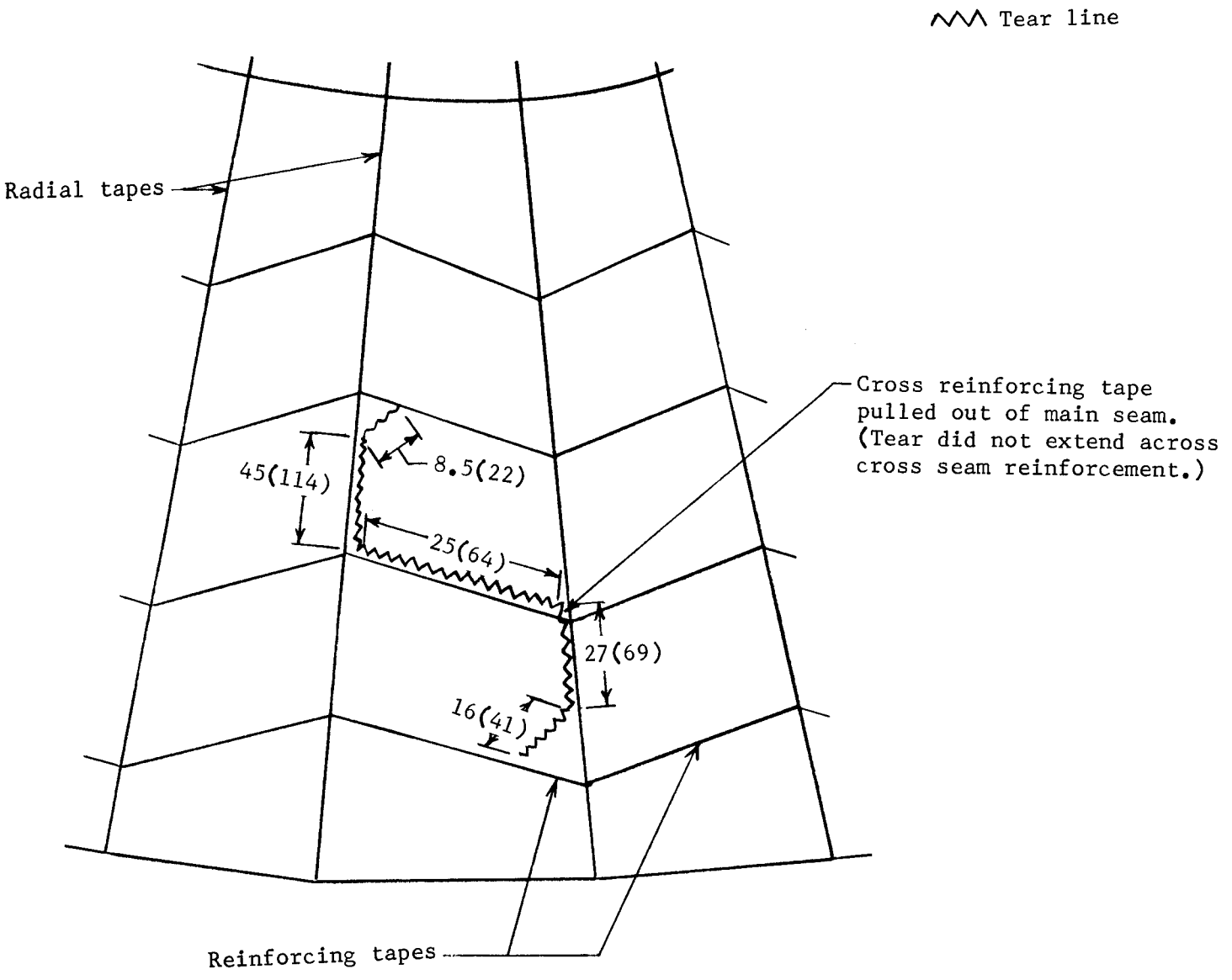

Figure 22.- Sketch of damaged section of parachute disk showing shape and size of tear. Dimensions are in inches (centimeters).